Spin Crossover in Novel Dihydrobis(1-pyrazolyl)borate [$H_2B(pz)_2$]-Containing Iron(II) Complexes. Synthesis, X-ray Structure, and Magnetic Properties of [$FeL\{H_2B(pz)_2\}_2$] (L = 1,10-Phenanthroline and 2,2′-Bipyridine)

José Antonio Real,*[1a] M. Carmen Muñoz,[1b] Juan Faus,[1a] and Xavier Solans[1c]

Departament de Química Inorgànica, Universitat de València, Dr. Moliner 50, 46100 Burjassot, València, Spain, Departament de Física Aplicada, Universidad Politécnica de València, Camino de Vera s/n, 46071, València, Spain, and Departament de Cristal.lografia, Mineralogia i Dipòsits Minerals, Facultat de Geologia, Universitat de Barcelona, 08028 Barcelona, Spain

Received August 8, 1996[⊗]

The first example of spin crossover iron(II) complexes based on dihydrobis(1-pyrazolyl)borate are presented here. The complexes {$Fe[H_2B(Pz)_2]_2$(phen)} (phen = 1,10-phenanthroline), **1**, and {$Fe[H_2B(Pz)_2]_2$(bipy)} (bipy = 2,2′-bipyridine), **2**, have been synthesized and their structures determined by X-ray diffraction methods. Crystals **1** and **2** are monoclinic, space group *C*2/*c*, $Z = 4$ with $a = 17.448(4)$ Å, $b = 16.101(4)$ Å, $c = 10.611(2)$ Å, and $\beta = 112.47(2)°$ for **1** and $a = 16.307(2)$ Å, $b = 15.075(4)$ Å, $c = 11.024(4)$ Å, and $\beta = 114.95(5)°$ for **2** at 293 K. The crystal structure of **2** was also determined at 139 K in order to detect the structural changes associated with the $S = 0 \leftrightarrow S = 2$ spin conversion. **2** retains the same space group upon spin conversion with $a = 16.086(6)$ Å, $b = 14.855(6)$ Å, $c = 10.812(2)$ Å, and $\beta = 114.18(3)°$. The structures of **1** and **2** are made up of mononuclear neutral species where the positive charge of iron(II) is neutralized through the coordination of two chelate bidentate dihydrobis(pyrazolyl)borate anions, and phen or bipy neutral ligands are used to fill the iron(II) coordination sphere. The molecular structures for both compounds are very similar, with Fe−N bond lengths in the 2.212−2.158 Å range for the high-spin phase. The structural modifications associated with the spin change in **2** mainly consist of a large reorganization of the metal environment: the Fe−N decreases by 0.15 Å (mean value) when the temperature is lowered from 290 to 139 K and a more regular shape of the [FeN_6] octahedron is achieved through a slight modification of the trigonal deformation angle from 5.3° to 3.2° along with remarkable variations of the N−Fe−N angles. The thermodynamic model of Slichter and Drickamer was applied to account for the magnetic data. The intermolecular interaction parameter and the enthapy and entropy changes associated with the spin transition were estimated as $\Gamma = 3.3$ kJ mol^{-1}, $\Delta H = 13.4$ kJ mol^{-1}, and $\Delta S = 81.9$ J mol^{-1} K^{-1} for **1** and $\Gamma = 1.7$ kJ mol^{-1}, $\Delta H = 13.4$ kJ mol^{-1}, and $\Delta S = 83.9$ J mol^{-1} K^{-1} for **2**, respectively.

Introduction

Electronic spin crossover phenomenon occurs in some six-coordinate first-row transition metal complexes as the result of an electronic instability driven by external constraints (temperature, pressure, or electromagnetic radiation)[2−4] that induce structural changes at molecular and lattice levels.[5] Six-coordinated iron(II) ($3d^6$) spin crossover compounds are among the most investigated systems; they reversibly change from diamagnetic ($S = 0$) to paramagnetic ($S = 2$) spin states. In the solid state, a cooperative first-order spin transition takes place at a well-defined temperature (T_c) for a few of these compounds, and this transition may show thermal hysteresis.

Although its grounds are well understood, the molecular factors which predispose the solid to undertake a discontinuous spin conversion is a problem which remains still open. Understanding of these factors is of utmost importance because of the potential use of spin crossover compounds in molecular-based electronic devices such as optical memory and switches.[6] The paucity of spin crossover compounds and the variety of magnetic behaviors that they exhibit make it very difficult to establish correlations between the nature of the spin transition and the molecular singularities. In an attempt to overcome these difficulties we undertake the present work which deals with the systematic synthesis of a new family of pyrazolylborate iron(II) complexes exhibiting spin crossover. Polypyrazolylborates were introduced into coordination chemistry by Trofimenko 28 years ago[7] and have been demonstrated to be very versatile ligands.[8] Long ago, Hutchinson *et al.* showed the suitability of these ligands to induce spin conversion in iron(II), particularly in the complex bis(hydro)tris(1-pyrazolyl)borate iron(II) and its parent bis(hydro)tris(3,5-dimethyl-1-pyrazolyl)borate iron(II), which are well-known spin crossover systems. The first one is low spin at room temperature and shows a spin state transition at T_c ca. 393 K, whereas the second is high spin at room temperature and shows a gradual spin state conversion between 245 and 194 K.[9]

⊗ Abstract published in *Advance ACS Abstracts,* June 1, 1997.

(1) (a) Departament de Química Inorgánica, Universitat de València. (b) Departament de Física Aplicada, Universitat Politécnica de Vàlencia. (c) Departament de Cristal.lografia, Mineralogia i Dipòsits Minerals, Facultat de Geologia, Universitat de Barcelona.
(2) (a) Gütlich, P. *Struct. Bonding (Berlin)* **1981**, *44*, 83. (b) Gütlich, P.; Hauser, A.; Spiering, H. *Angew. Chem., Int. Ed. Engl*. **1994**, *33*, 2024.
(3) König, E. *Struct. Bonding (Berlin)* **1991**, *76*, 51.
(4) Gütlich, P.; Hauser, A. *Coord. Chem. Rev*. **1990**, *97*, 1.
(5) König, E. *Progr. Inorg. Chem*. **1987**, *35*, 527.
(6) (a) Decurtins, S.; Gütlich, P.; Köhler, C. P.; Spiering, H.; Hauser, A. *Chem. Phys. Lett*. **1984**, *105*, 1. (b) Roux, C.; Zarembowitch, J.; Gallois, B.; Granier, T.; Claude, R. *Inorg. Chem*. **1994**, *33*, 2273. (c) Kahn, O.; Kröber, J.; Jay, C. *Adv. Mater*. **1992**, *4*, 718.
(7) Trofimenko, S. *J. Am. Chem. Soc*. **1967**, *89*, 3170.
(8) (a) Trofimenko, S. *Chem. Rev*. **1993**, *93*, 943. (b) Trofimenko, S. *Prog. Inorg. Chem*. **1986**, *39*, 115.
(9) (a) Hutchinson, B. B.; Daniels, L.; Henderson, E.; Neill, P. *J. Chem. Soc., Chem. Commun*. **1979**, 1003. (b) Olivier, J. D.; Mullica, D. F.; Hutchinson, B. B.; Milligan, W. O. *Inorg. Chem*. **1980**, *19*, 165. (c) Long, G. J.; Hutchinson, B. B. *Inorg. Chem*. **1987**, *26*, 608.

S0020-1669(96)00965-2 CCC: $14.00

Chart 1

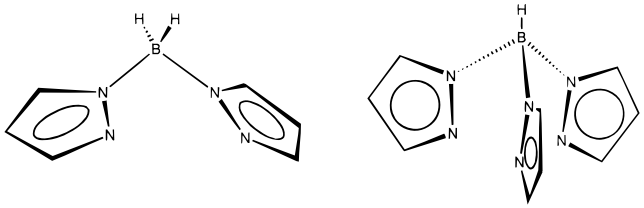

(a) (b)

Hydrotris(1-pyrazolyl)borate [$HB(Pz)_3^-$] usually behaves as a tridentate ligand (see Chart 1b) forming very stable octahedral "sandwich" complexes with divalent first-row transition metal ions. This is a serious difficulty aiming at synthesizing new mixed-ligand complexes containing this kind of anionic chelating ligands. However, the dihydrobis(1-pyrazolyl) [$HB(Pz)_2^-$] homologue (see Chart 1a) is a priori a better candidate because of its bidentate coordination mode.

The positive charge of iron(II) is neutralized through the coordination of two dihydrobis(1-pyrazolyl)borate ligands, and the two remaining coordination sites can be filled by one neutral bidentate ligand such as phenanthroline (phen) or bipyridine (bipy) or by two monodentate ones such as triazole, pyrazole, or pyridine.

As a first step in this direction we report in the present work on the synthesis, single crystal X-ray structure, and magnetic properties of $\{Fe[H_2B(Pz)_2]_2(L)\}$ compounds with L = phen (**1**) and bipy (**2**).

Experimental Section

Synthesis of 1 and 2. To a solution of $KH_2B(Pz)_2$ (2 mmol) in MeOH (10 cm^3) was added a solution of $Fe(ClO_4)_2 \cdot 6H_2O$ (1 mmol) in the same solvent (5 mL). The mixture was stirred for 10 min, decanted off, and filtered. The precipitate of potassium perchlorate was washed with 5 mL of MeOH. The methanolic fractions containing $[Fe(H_2B(pz)_2)_2]$ were collected, and solutions of phen or bipy (1 mmol) in MeOH (10 mL) were added dropwise to the resulting uncolored iron(II)-containing solution. A pink-violet crystalline product formed immediately, which is filtered, washed with MeOH, and dried. All the manipulations were carried out under argon atmosphere. Anal. Calcd for $C_{24}H_{24}N_{10}B_2Fe$: C, 54.34; H, 4.50; N, 26.45. Found: C, 54.1; H, 4.2; N, 26.1. Anal. Calcd for $C_{22}H_{24}N_{10}B_2Fe$: C, 52.17; H, 4.74; N, 27.67. Found: C, 51.6; H, 4.6; N, 27.3.

Single crystals of **1** and **2** were obtained by slow diffusion in MeOH under argon atmosphere, using a H double-tube glass vessel. The starting materials were on one arm a methanolic solution of phen or bipy, and on the other arm a methanolic solution of $[Fe(H_2B(pz)_2)_2]$. Pink-violet single crystals formed after 2 weeks and were collected, washed in MeOH, and dried in an argon stream.

Magnetic Susceptibility Measurements. The variable-temperature magnetic susceptibility measurements were carried out on polycrystalline samples over the temperature range 4.2−300 K with a fully automatized AZTEC DSM8 pendulum-type susceptometer equipped with a TBT continuous-flow cryostat and a Brüker BE15 electromagnet, operating at 1.8 T. The apparatus was calibrated with mercury tetrakis(thiocyanato)cobaltate(II). Experimental susceptibilities were corrected for diamagnetism of the constituent atoms by the use of Pascal's constants.

Solution and Refinement of the X-ray Structures. Concerning compound **2**, low-temperature X-ray diffraction experiments were conducted by cooling the sample with a cold nitrogen gas flow surrounded by a jacket of dry nitrogen gas at room temperature, which prevents frost from growing around the sample. Data collections were carried out on an Enraf-Nonius CAD4 diffractometer with monochromatized Mo Kα radiation ($\lambda = 0.710\ 73$ Å). Details concerning crystal data, data collection characteristics, and structure refinement are summarized in Table 1. Lattice parameters were obtained from least-squares refinement of the setting angles of 25 reflections in the range $15 < \theta < 25°$. Lorentz-polarization correction was applied, but no absorption corrections were made. **1** and **2** were solved by direct methods using SHELX86[10] and refined by full least-squares refinement using SHELX76.[11] Atomic scattering factors were taken from ref 12. The final full-matrix least-squares refinement, minimizing the function $\Sigma w(F_o - F_c)^2$ (each reflection being assigned a unit weight), converged to R and $R_w = 0.037$, 0.076 for the room- and low-temperature structures of **2**. Concerning the room-temperature structure of **1**, final reliability factors were R and $R_w = 0.042$. Non-hydrogen atoms were refined anisotropically for both compounds. All hydrogen atoms were placed in computed positions and isotropically refined. Fractional atomic coordinates for **1** and **2** are given in Tables 2−4.

Tables of anisotropic thermal parameters of non-hydrogen atoms, hydrogen coordinates, and least-squares planes are deposited as Supporting Information (Tables S1−S9).

Table 1. Crystallographic Data and Experimental Parameters for **1** and **2**

		2	
	1	(293 K)	(139 K)
empirical formula	$C_{24}H_{24}N_{10}B_2Fe$	$C_{22}H_{24}N_{10}B_2Fe$	$C_{22}H_{24}N_{10}B_2Fe$
formula wt	529.99	505.97	505.97
cryst color, habit	pink-violet, prismatic	pink-violet, prismatic	pink-violet
cryst dimens (mm)	0.4 × 0.3 × 0.3	0.3 × 0.3 × 0.2	0.2 × 0.3 × 0.2
cryst system	monoclinic	monoclinic	monoclinic
lattice params			
a, Å	17.448(4)	16.307(2)	16.086(6)
b, Å	16.101(4)	15.075(4)	14.855(2)
c, Å	10.611(2)	11.024(4)	10.812(2)
β, deg	112.47(2)	114.95(5)	114.18(3)
V, Å^3	2543(1)	2462(2)	2356(1)
space group	*C*2/*c*	*C*2/*c*	*C*2/*c*
Z value	4	4	4
ρ_{calc} (g/cm^3)	1.385	1.365	1.426
μ(Mo Kα) (cm^{-1})	11.86	12.25	6.73
no. of observations	1539 ($I > 3\sigma(I)$)	1884 ($I > 3\sigma(I)$)	2301
no. of valiables	171	162	208
residuals: $R = R_w$[a]	0.042	0.037	0.056

[a] $R = \Sigma(||F_o| - |F_c||)/\Sigma|F_o|$.

Table 2. Atomic Coordinates and Equivalent Isotropic Thermal Parameters (Å^2 × 10^3) for Compound **1**

	x/*a*	*y*/*b*	*z*/*c*	U_{eq}
Fe	0.50000	0.23925(5)	0.25000	42.2(5)
B	0.4737(4)	0.3148(4)	−0.0804(6)	68(3)
N1	0.4300(2)	0.1303(2)	0.1094(4)	48(2)
N2	0.5886(2)	0.2426(2)	0.1620(3)	49(2)
N3	0.4162(2)	0.3335(2)	0.0936(4)	48(2)
N4	0.5709(2)	0.2873(2)	0.0410(4)	55(2)
N5	0.4302(2)	0.3653(2)	−0.0111(4)	56(2)
C1	0.3645(3)	0.1316(3)	−0.0307(5)	62(3)
C2	0.3297(4)	0.0597(4)	−0.1155(6)	77(3)
C3	0.3617(4)	−0.0155(4)	−0.0526(7)	85(3)
C4	0.4306(4)	−0.0196(3)	0.0978(6)	74(3)
C5	0.4634(3)	0.0559(2)	0.1734(5)	53(3)
C6	0.4663(4)	−0.0951(3)	0.1727(7)	101(3)
C7	0.6757(3)	0.2207(3)	0.2293(5)	57(3)
C8	0.7131(3)	0.2500(3)	0.1515(5)	69(3)
C9	0.6452(3)	0.2921(3)	0.0334(5)	68(3)
C10	0.3936(4)	0.4409(3)	−0.0496(6)	80(3)
C11	0.3550(4)	0.4600(3)	0.0285(6)	85(3)
C12	0.3706(3)	0.3911(3)	0.1176(5)	63(3)

(10) Sheldrick, G. M. SHELX-86, Program for Structure Determination, University of Gottingen, FRG, 1986.
(11) Sheldrick, G. M. System of Computing Programs, University of Cambridge, Cambridge, England, 1976.
(12) *International Tables for X-ray Crystallography*; Kinoch Press: Birmingham, England, 1974; Vol. 4, p 99.

Table 3. Atomic Coordinates and Equivalent Isotropic Thermal Parameters ($Å^2 \times 10^3$) for Compound **2** at 293 K

	x/*a*	*y*/*b*	*z*/*c*	U_{eq}
Fe	0.00000	0.22918(3)	0.25000	39.0(3)
B	0.0190(2)	0.2935(3)	−0.0422(3)	59.3(9)
N1	−0.0619(2)	0.1113(2)	0.1251(2)	47.0(9)
N2	0.1138(1)	0.2336(2)	0.1941(2)	45.3(9)
N3	−0.0672(2)	0.3281(2)	0.0991(2)	47.9(8)
N4	0.1099(2)	0.2759(2)	0.0827(2)	50.2(8)
N5	−0.0436(2)	0.3514(2)	−0.0012(2)	48.9(8)
C1	−0.1234(2)	0.1160(2)	−0.0025(3)	58.0(9)
C2	−0.1580(2)	0.0408(2)	−0.0803(3)	69(1)
C3	−0.1303(3)	−0.0389(3)	−0.0256(4)	84(1)
C4	−0.0681(2)	−0.0459(2)	0.1061(4)	73(1)
C5	−0.0341(2)	0.0311(2)	0.1798(3)	53(1)
C6	0.2018(2)	0.2191(2)	0.2697(3)	50(1)
C7	0.2544(2)	0.2505(2)	0.2078(3)	60(1)
C8	0.1937(2)	0.2866(2)	0.090893)	62(1)
C9	−0.1231(2)	0.3913(2)	0.1035(3)	58(1)
C10	−0.1369(2)	0.4546(2)	0.0055(4)	68(1)
C11	−0.0858(2)	0.4270(2)	−0.0582(3)	64(1)

Table 4. Atomic Coordinates and Equivalent Isotropic Thermal Parameters ($Å^2 \times 10^3$) for Compound **2** at 139 K

	x/*a*	*y*/*b*	*z*/*c*	U_{eq}
Fe	0.50000	0.2711(1)	0.25000	19(1)
B	0.5207(2)	0.2029(2)	−0.0406(3)	30(1)
N1	0.4427(1)	0.3757(1)	0.1259(2)	23(1)
N2	0.6087(1)	0.2687(1)	0.1979(2)	22(1)
N3	0.4385(1)	0.1716(1)	0.1130(2)	25(1)
N4	0.6083(1)	0.2263(1)	0.0865(2)	26(1)
N5	0.4570(1)	0.1467(1)	0.0054(2)	27(1)
C1	0.3810(2)	0.3698(2)	−0.0038(3)	29(1)
C2	0.3456(2)	0.4454(2)	−0.0846(3)	37(1)
C3	0.3710(2)	0.5213(2)	−0.0287()	41(1)
C4	0.4322(2)	0.5389(2)	0.1025(3)	37(1)
C5	0.4674(2)	0.4603(1)	0.1798(2)	27(1)
C6	0.6964(2)	0.2895(2)	0.2762(2)	28(1)
C7	0.7508(2)	0.2608(2)	0.2125(3)	34(1)
C8	0.6942(2)	0.2197(2)	0.0959(3)	32(1)
C9	0.3798(2)	0.1078(2)	0.1197(3)	33(1)
C10	0.3611(2)	0.0438(2)	0.0191(3)	40(1)
C11	0.4103(2)	0.0707(2)	−0.0533(3)	35(1)

Results

Description of the Structures. Structures of 1 and 2 at 290 K. Compounds **1** and **2** crystallize in the monoclinic *C*2/*c* space group. The molecules are chiral, and the unit cell contains two right-handed and two left-handed [Fe($H_2B(Pz)_2$)L] enantiomers. Each iron is sourrounded by six nitrogen atoms belonging to two $H_2B(Pz)_2^-$ ligands and one phen or bipy group for **1** or **2**, respectively. Both $H_2B(Pz)_2^-$ anions are in *cis* position to each other. Figures 1 and 2 show a perspective drawing of **1** and **2**, respectively, together with the atom-numbering scheme. Selected interatomic distances and bond angles are displayed in Tables 5−7.

The ligands phen and bipy are nearly planar, defining their least-squares planes by the position of their central atoms N(1), C(5), C(4), N(1)′, C(5)′, C(4)′ (equation plane $-16.7X + 0.0Y + 7.9Z = -6.3$ for phen and $15.5X + 0.0Y - 7.5Z = -1.9$ for bipy); the largest deviations observed are 0.052 Å (N(1)) and −0.024 Å (N(1)) for phen and bipy, respectively. The boron atom is approximately in a tetrahedral environment, as expected (HBH, HBN, and NBN angles are found within the 109−110.5° range). Dihedral angles formed between the planes N(4), N(5), B and N(2), N(3), Fe with respect to the plane N(2), N(3), N(4), N(5) are 47.0° and 4.1° for compound **1** and 46.3° and 10.9° for compound **2**, respectively. Consequently, the boron and iron atoms lie 0.65 and 0.1 Å for **1** and 0.65 Å and 0.30 Å for **2** above the same plane, respectively (see Chart 2). The distance between iron(II) ion and boron atom through the six-membered chelate ring is 3.5 Å for both compounds. The pyrazole rings are planar, as expected (deviations from the mean planes not greater than 0.004 Å), and define dihedral angles with respect to the plane N(4), N(5), N(3), N(2): 26.4° [pyrazole (1), pz-(1)] and 18.7° [pyrazole (2), pz(2)] for **1** and 25.3° [pz(1)] and 22.5° [pz(2)] for **2**.

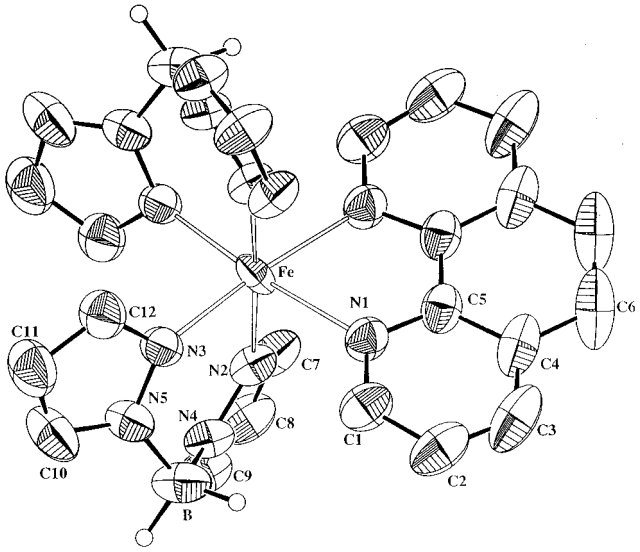

Figure 1. Perspective drawing of [Fe{$H_2B(Pz)_2$}$_2$phen] with the atom-numbering scheme.

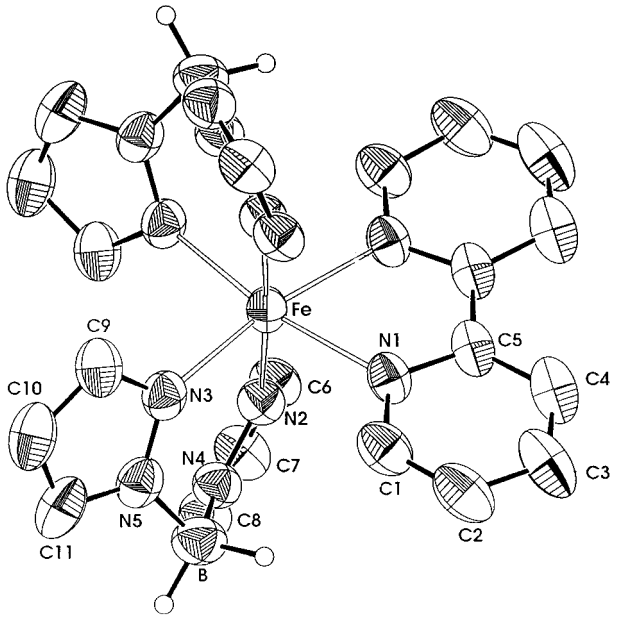

Figure 2. Perspective drawing of [Fe{$H_2B(Pz)_2$}$_2$bipy] with the atom-numbering scheme.

The [FeN_6] octahedron geometry defined by the six nitrogen atoms around the iron(II) ion has no regular shape. The Fe−N bond lengths for the asymmetric unit Fe−N(1), Fe−N(2), and Fe−N(3) are 2.212, 2.184, and 2.158 Å for **1** and 2.213, 2.190, and 2.157 Å for **2**, respectively. The coordination sphere can be considered as a compressed octahedron, since Fe−N(3) and Fe−N(3′) lengths are significantly shorter than the other four Fe−N distances. Moreover, the geometric constraints of the phen ligand in **1** and the bipy ligand in **2** cause important reduction of the N(1)−Fe−N(1′) bite angle from the ideal 90° value: 75.03° and 73.21° for **1** and **2**, respectively. The magnitude of the trigonal distortion angle Φ is 4.6° and 5.3°

Table 5. Selected Bond Distances (Å) and Bond Angles (deg) for Compound **1**[a]

N1−Fe	2.212 (3)	N1−Fe−N3	97.2 (1)
N2−Fe	2.184 (3)	N1−Fe−N2	89.8 (1)
N3−Fe	2.158 (3)	N2−Fe−N3	90.9 (1)
B−N4	1.566 (6)	N1−Fe−N1′	75.0 (1)
B−N5	1.536 (6)	N3−Fe−N3′	90.7 (1)
		N4−B−N5	110.4 (3)
	Pyrazole 1		
N5−N3	1.357 (4)	C12−N3−N5	106.0 (3)
C12−N3	1.331 (5)	C11−C12−N3	110.5 (4)
C10−N5	1.336 (6)	C20−N5−N3	109.4 (4)
C10−C11	1.348 (7)	C10−C11−C12	104.6 (4)
C11−C12	1.390 (6)	C11−C1−N5	109.5 (4)
	Pyrazole 2		
N4−N2	1.360 (4)	C7−N2−N4	106.0 (3)
C7−N2	1.346 (5)	C9−N4−N2	109.7 (4)
C9−N4	1.342 (5)	C8−C7−N2	110.5 (4)
C8−C7	1.376 (6)	C9−C8−C7	105.3 (4)
C9−C8	1.372 (6)	C8−C9−N4	108.5 (4)
		Hb1−B−Hb2	109.5 (4)
	Phen		
C1−N1	1.320 (5)	C1−N1−C5	118.2 (4)
C5−N1	1.350 (5)	C2−C1−N1	122.9 (5)
C2−C1	1.395 (6)	C3−C2−C1	119.7 (5)
C3−C2	1.354 (7)	C2−C3−C4	119.2 (4)
C3−C4	1.412 (7)	C3−C4−C5	117.2 (5)
C4−C5	1.403 (6)	C4−C5−N1	122.8 (4)

[a] Symmetry transformation used to generate equivalent atoms (′): $-x + 1, y, -z + {}^1/_2$.

Table 6. Selected Bond Distances (Å) and Bond Angles (deg) for Compound **2** (293 K)[a]

N1−Fe	2.213 (2)	N1−Fe−N2	93.9 (1)
N2−Fe	2.190 (2)	N3−Fe−N1	97.2 (1)
N3−Fe	2.157 (2)	N3−Fe−N2	88.7 (1)
B−N4	1.562 (4)	N1−Fe−N1′	73.2 (1)
B−N5	1.549 (4)	N3−Fe−N3′	92.6 (1)
		N5−B−N4	109.6 (2)
	Pyrazole 1		
N5−N3	1.361 (3)	C9−N3−N5	106.1 (2)
C9−N3	1.334 (3)	C11−N5−N3	109.5 (2)
C11−N5	1.343 (4)	C10−C9−N3	110.6 (3)
C10−C9	1.387 (4)	C9−C10−C11	105.0 (3)
C10−C11	1.362 (5)	C10−C11−N5	108.8 (3)
	Pyrazole 2		
N4−N2	1.361 (3)	C6−N2−N4	105.6 (2)
C6−N2	1.339 (3)	C8−N4−N2	109.8 (2)
C8−N4	1.342 (3)	C7−C6−N2	111.1 (2)
C7−C6	1.385 (4)	C8−C7−C6	104.5 (3)
C7−C8	1.364 (4)	C7−C8−N4	109.2 (3)
		Hb2−B−Hb1	109.5 (3)
	Bipy		
C1−N1	1.342 (3)	C1−N1−C5	118.7 (2)
C5−N1	1.343 (3)	C2−C1−N1	122.3 (3)
C2−C1	1.389 (4)	C3−C2−C1	118.9 (3)
C3−C2	1.335 (5)	C4−C3−C2	120.2 (3)
C3−C4	1.380 (5)	C3−C4−C5	119.1 (3)
C4−C5	1.391 (4)	C4−C5−N1	120.9 (3)

[a] Symmetry transformation used to generate equivalent atoms (′): $-x, y, -z + {}^1/_2$.

for **1** and **2**, respectively (a value of 0° is expected for a regular octahedron).

Short interligand contacts within the complex units are observed for the atoms [C(7) and C(6)] (for **1** and **2**, respectively) of pz(2), and B with respect to C(1) (phen or bipy rings) being 3.661 and 3.688 Å for **1** and 3.888 and 3.695 Å for **2**, respectively.

Structure of 2 at 139 K. The structure was refined in the *C*2/*c* monoclinic space group. No drastic change is observed

Table 7. Selected Bond Distances (Å) and Bond Angles (deg) for Compound **2** (139 K)[a]

N1−Fe	2.013 (2)	N1−Fe−N2	92.28 (7)
N2−Fe	2.046 (2)	N3−Fe−N1	96.99 (8)
N3−Fe	2.039 (2)	N3−Fe−N2	90.13 (8)
B−N4	1.552 (3)	N1−Fe−N1′	78.94 (11)
B−N5	1.553 (3)	N3−Fe−N3′	87.08 (10)
		N5−B−N4	108.4 (2)
	Pyrazole 1		
N5−N3	1.364 (3)	C9−N3−N5	104.8 (2)
C9−N3	1.362 (3)	C11−N5−N3	110.5 (2)
C11−N5	1.361 (3)	C10−C9−N3	111.6 (2)
C10−C9	1.381 (4)	C9−C10−C11	104.9 (2)
C10−C11	1.381 (4)	C10−C11−N5	108.1 (2)
	Pyrazole 2		
N4−N2	1.357 (3)	C6−N2−N4	106.7 (2)
C6−N2	1.351 (3)	C8−N4−N2	109.5 (2)
C8−N4	1.348 (3)	C7−C6−N2	111.1 (2)
C7−C6	1.384 (4)	C8−C7−C6	106.3 (2)
C7−C8	1.360 (4)	C7−C8−N4	108.3 (2)
		Hb2−B−Hb1	128.0 (2)
	Bipy		
C1−N1	1.348 (3)	C1−N1−C5	117.5 (2)
C5−N1	1.374 (3)	C2−C1−N1	122.5 (2)
C2−C1	1.393 (3)	C3−C2−C1	119.5 (2)
C3−C2	1.400 (4)	C4−C3−C2	119.0 (2)
C3−C4	1.360 (4)	C3−C4−C5	119.5 (2)
C4−C5	1.413 (3)	C4−C5−N1	121.9 (2)

[a] Symmetry transformation used to generate equivalent atoms (′): $-x + 1, y, -z + {}^1/_2$.

Chart 2

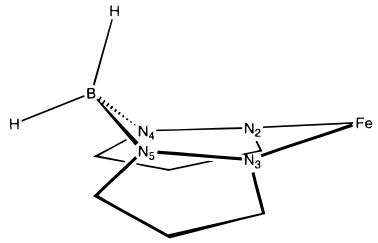

in the molecular configuration of the $[Fe(H_2B(Pyrazole)_2)_2$-(bipy)] unit. The most important change concerns the $[FeN_6]$ octahedron geometry.

Dihedral angles defined by planes N(4), N(5), B and N(2), N(3), Fe with respect to the plane N(5), N(3), N(4), N(5) are 41.0° and 13.3°. Consequently, the boron and iron atoms lie 0.65 and 0.33 Å above this plane, respectively. The bending angles defined by the pyrazole rings with respect to the N(2), N(3), N(4), N(5) plane are 21.5° and 22.8° for pz1 and pz2, respectively.

Fe−N bond lengths are shorter than those observed at room temperature: 2.013, 2.039, and 2.046 Å for Fe−N(1), Fe−N(3), and Fe−N(2), respectively. That implies an average Fe−N shortening of 0.152 Å. The bite angle of the bipy ligand, N(1)−Fe−N(1′), increases significantly, attaining a value of 78.94°. The trigonal distortion angle changes to a lower value, 3.18°. At low temperature, intramolecular constraints become more severe than at room temperature: distances from C(6), pz(2) and B to C(1) are 3.39 and 3.477 Å, respectively.

Magnetic Measurements. The temperature dependence of the $\chi_M T$ product (χ_m = molar magnetic susceptibility, T = temperature) for microcrystalline samples of **1** and **2** is displayed in Figure 3. The $\chi_m T$ value for both compounds at room temperature is 3.6 $cm^3\ mol^{-1}$ K, which corresponds to what is expected for a high-spin iron(II) ion. This value slowly decreases upon cooling ($\chi_M T$ = 3.36 $cm^3\ mol^{-1}$ K at 165 K). In the temperature range (165−155 K) the $\chi_M T$ product for **1**

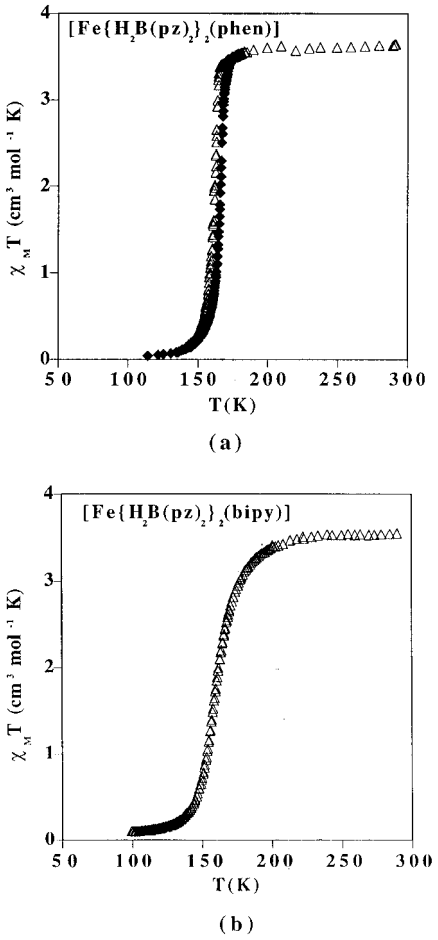

Figure 3. Temperature variation of $\chi_m T$ for [Fe{$H_2B(Pz)_2$}$_2$phen] (a), and [Fe{$H_2B(Pz)_2$}$_2$bipy] (b).

suddenly decreases to a practically vanishing value (0.08 cm^3 mol^{-1} K), which corresponds to low-spin iron(II). The warming mode reveals a thermal hysteresis of ca. 4 K, the T_c value on cooling and warming modes being 161.8 and 165.6, respectively (7 h to run the full hysteresis loop, i.e. 10−15 min K^{-1}), and 70% of the spin conversion occurs within an interval of 6 K. All of these features are indicative of a strongly cooperative first-order spin transition. Compound **2** behaves in a similar way, but the spin conversion is more gradual, shows no detectable thermal hysteresis, and is centered around $T_c = 160$ K.

Discussion

The molecular structures of **1** and **2** show that both compounds have similar pseudo-octahedral coordination cores. The corresponding metal−ligand distances of the two complexes, at room temperature, are very similar. The mean values relative to Fe−N[$H_2B(Pz)_2^-$] being 2.171 and 2.173 Å and those relative to Fe−N(phen, bipy) being 2.212 and 2.213 Å (the average value of the [FeN_6] bond distances is 2.184 and 2.186 Å) for **1** and **2**, respectively. It should be noted that the above-mentioned mean distances compare with those found in analogous spin crossover compounds of general formula [Fe$(L)_2(NCS)_2$], where L = bipy, 2.133 Å,[13] phen, 2.156 Å,[14] btz, 2.135 Å,[15] tap, 2.162 Å,[16] and bt, 2.158 Å[17] (where, btz, tap, and bt are 2,2′-bi-4,5-dihydrothiazine, 1,4,5,8-tetraazaphenanthrene, and 2,2′-bithiazoline, respectively). More precisely, the average Fe−N(phen) and Fe−N(bipy) distance in Fe$(phen)_2(NCS)_2$ and Fe$(bipy)_2$-$(NCS)_2$ is 2.206 and 2.173 Å, respectively.

Dihydrobis(pyrazolyl)borate adopts unsymmetrical conformation with respect to the average N(2)−N(3)−N(4)−N(5) plane. The dihedral angle defined with pyrazole rings (pz) are different in both compounds, being smaller for pz(2):

pz(1) 26.4°, pz(2) 18.7° for **1**

pz(1) 25.3°, pz(2) 22.5° for **2**

Furthermore, the dihedral angle defined by N(2)−N(3)−Fe and N(2)−N(3)−N(4)−N(5) planes is significantly smaller for **1** (4.11°) than for **2** (10.9°). Consequently, the iron atom remains out of the plane containing the four nitrogen atoms by 0.1 and 0.33 Å for **1** and **2**, respectively. All these facts probably are determined by the observed C(1)[phen, bipy]···[C(7), C(6)] [pz-(2)] short intramolecular interligand contacts (C(1)···C(7) = 3.661 Å for **1** and C(1)···C(6) = 3.888 Å for **2**). It is known that dihydrobis(pyrazolyl)borate ligand attains a degree of flexibility through rotation of the pyrazole rings about the N−N vector.[18] And also that such a rotation is accompanied by a more or less pronounced flattening of the boat conformation of the six-membered chelate ring, mainly at the metal site.

The X-ray structure of the low-spin phase for compound **1** could not be done because the crystal cracks at temperatures below T_c, in contrast with **2**. The most conspicuous variations accompanying the spin state conversion in **2** concern the metal−ligand bond lengths. The mean value of this variation is found to be 0.154 Å, which lies within the expected range for $S = 2 \leftrightarrow S = 0$ conversions in the iron(II) spin crossover compounds having a [FeN_6] coordination core.[19] The larger decrease observed for Fe−N(bipy) distances (∼0.20 Å) as compared with Fe−N[$H_2B(Pz)_2^-$] distances (∼0.13 Å) when passing from the high- to the low-spin form may be mainly accounted for by the fact that 2,2′-bipyridine ligand acts as a better π-electron acceptor than the [$H_2B(Pz)_2^-$] group. So, in the low-spin isomer the electron back-donation from filled metal π orbitals to vacant π^* ligand orbitals is expected to be more important for bipy than for [$H_2B(Pz)_2^-$], which results in a higher strengthening of Fe−N(bipy) with regard to Fe−N[$H_2B(Pz)_2^-$] bonds.

As far as the N−Fe−N angles are concerned, significant increasing (+5.7°) and decreasing (−5.5°) variations are observed on going from room temperature to 139 K for N(1)−Fe−N(1′) and N(3)−Fe−N(3′) angles, respectively. The variation of the N(1)−Fe−N(1′) angle is caused by the strengthening of the Fe−N(bipy) distances. The negative variation of the angle N(3)−Fe−N(3′) is likely due to two effects: increasing of the N(1)−Fe−N(1′) angle and avoiding the above-mentioned short contact between C(6)[pz(2)] and C(1)[bipy]. Moreover, the dihedral angles defined by the planes pz(1) and N(2), N(3), Fe with respect to the plane N(2), N(3), N(4), N(5) change upon spin conversion by −4° and +2.2°, respectively. Another relevant angular parameter is the trigonal distortion angle. Most of the iron(II) spin crossover complexes have pseudo-octahedral cores in the high-spin state; hence the trigonal distortion angle is $\Phi \neq 0$. There is sufficient experimental data to suggest that

(13) Konno, M.; Mikami-Kido, M. *Bull. Chem. Soc. Jpn.* **1991**, *64*, 339.
(14) Gallois, B.; Real, J. A.; Hauw, C.; Zarembowitch, J. *Inorg. Chem.* **1990**, *20*, 1152.
(15) Real, J. A.; Gallois, B.; Granier, T.; Suez-Panamá, F.; Zarembowitch, J. *Inorg. Chem.* **1992**, *31*, 4972.
(16) Real, J. A.; Muñoz, M. C.; Andrés, E.; Granier, T.; Gallois, B. *Inorg. Chem.* **1994**, *33*, 3587.
(17) Ozarowski, A.; McGarvey, B. R.; Sarkar, A. B.; Drake, J. E. *Inorg. Chem.* **1988**, *27*, 628.
(18) (a) Dapporto, P.; Mani, F.; Mealli, C. *Inorg. Chem.* **1978**, *17*, 1323. (b) Kokusen, H.; Sohrin, Y.; Matsui, M.; Hata, Y.; Hasegawa, H. *J. Chem. Soc., Dalton Trans.* **1996**, 195.
(19) König, E. *Prog. Inorg. Chem.* **1987**, *35*, 527.

Φ is coupled with the degree of spin conversion[20] and that both the trigonal twist and the radial movements are synchronous. The trigonal distortion angle decreases slightly upon spin conversion from 5.3° to 3.18° for **2**. The Φ high-spin value and the difference, $\Delta\Phi$, between high- and low-spin forms for compound **2** are considerably smaller than those of the $Fe(L)_2(NCS)_2$ family.[16]

Regarding the magnetic properties of **1** and **2**, they clearly show abrupt spin conversion. A discontinuous spin conversion is indicative of a greater cooperativity than a continuous one. So, a simple Gibbs−Boltzmann distribution for molecules in the low-spin state and thermally accessible high-spin excited state cannot account for the spin conversion. In such a situation, the thermodynamical parameters associated with the spin crossover process can be estimated applying the model of Slichter and Drickamer.[21] This model is based on the assumption that high-spin and low-spin molecules are statistically distributed and form regular solutions. At equilibrium, this model leads to the implicit equation

$$\ln\left(\frac{1-c}{c}\right) = \frac{\Delta H + \Gamma(1-2c)}{RT} - \frac{\Delta S}{R} \qquad (1)$$

Here, Γ is a term that reflects the strength of the cooperative intermolecular interactions. The high-spin molar fraction, c, is calculated at each temperature from the magnetic measurements using

$$c = [\chi_m T - (\chi_m T)_{ls}]/[(\chi_m T)_{hs} - (\chi_m T)_{ls}] \qquad (2)$$

Values of $\chi_m T$ for the pure high-spin (hs) and low-spin (ls) forms are directly obtained from the magnetic data, since the spin conversion is completed. A least-squares fit of the experimental data yields $\Delta H = 13.4$ kJ mol^{-1}, $\Gamma = 1.7$ kJ mol^{-1}, and $\Delta S = 83.9$ J mol^{-1} K^{-1} for **2** (see Figure 4). The agreement factor defined as $\sum_i[(T)_{exp,i} - (T)_{calc,i}]^2/\sum_i[T_{exp,i}]^2$ is 7×10^{-5}. A similar least-squares analysis is not appropiate for **1** given that Slichter and Drickamer's model can only account for the amplitude of the hysteresis loop. So, keeping in mind that ΔH and ΔS values for **1** must be very close to those found for compound **2**, and considering that the two "vertical" tangents of the calculated curve must cross the experimental hysteresis branches at the inflexion point, the simulation of the magnetic behavior of **1** with the parameters $\Delta H = 13.4$ kJ mol^{-1}, $\Gamma = 3.3$ kJ mol^{-1}, and $\Delta S = 81.9$ J mol^{-1} is possible (see Figure 5). The ΔH and ΔS values estimated for **1** and **2** are close to those found for other iron(II) spin crossover complexes.[22]

In summary, the major point of the present work is that the dihydrobis(pyrazolyl)borate iron(II) complexes are a new family of spin crossover complexes on which a large variety of chemical changes (replacement of C−H groups in the pyrazolyl units by nitrogen atoms affording dihydrobis(triazolyl) and -(tetrazolyl) borates, substitution of phen or bipy by others chelating or monodentate bridging and nonbridging ligands) can be carried out, offering the possibility to investigate systematically their effects on the cooperative mechanism. Much effort will be concentrated on this subject.

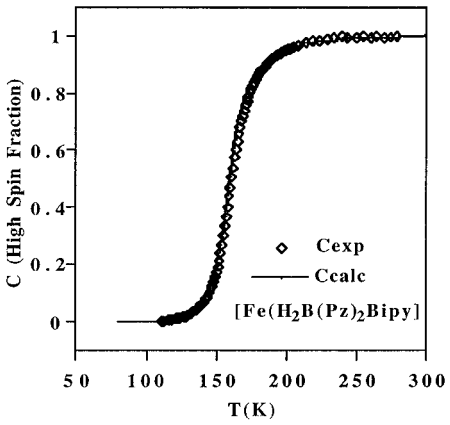

Figure 4. Experimental and simulated (full line) high-spin molar fraction vs T curves for $[Fe\{H_2B(Pz)_2\}_2bipy]$.

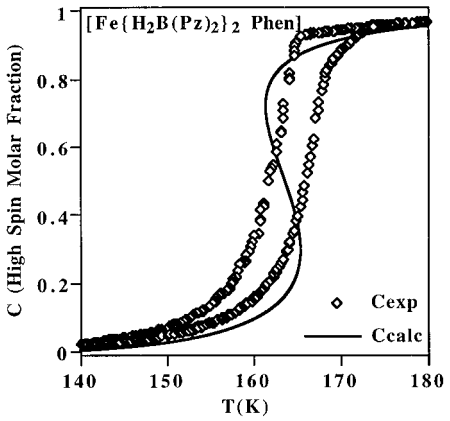

Figure 5. Experimental and simulated (full line) high-spin molar fraction vs T curves for $[Fe\{H_2B(Pz)_2\}_2phen]$.

Acknowledgment. We thank for financial support the Dirección General de Investigación Científica y Técnica (DGICYT) (Spain) through Project PB95-1002, and the Human Capital and Mobility Program (Network on Magnetic Molecular Materials from EEC) through Grant ERBCHRXCT920080.

Supporting Information Available: Tables S1−S9, giving anisotropic thermal parameters, hydrogen atom locations, and least-squares planes (9 pages). Ordering information is given on any current masthead page.

IC960965C

(20) (a) See ref 16. (b) Chang, H. R.; McCuster, J. K.; Toftlund, H.; Wilson, R. S.; Trautwein, A. X.; Winkler, H.; Hendrickson, D. N. *J. Am. Chem. Soc.* **1990**, *112*, 6814. (c) Purcell, K. F. *J. Am. Chem. Soc*. **1979**, *101*, 5147.
(21) Slichter, C. P.; Drickamer, H. G. *J. Chem. Phys* **1972**, *56*, 2142.
(22) (a) See ref 3. (b) McGarvey, J. J.; Lawthers, I.; Heremans, K.; Toftlund, H. *Inorg. Chem.* **1990**, *29*, 252.